Ultrastructural Pathology

ISSN: 0191-3123 (Print) 1521-0758 (Online) Journal homepage: https://www.tandfonline.com/loi/iusp20

Ultrastructural Characterization of Genetic Diffuse Lung Diseases in Infants and Children: A Cohort Study and Review

Arianna Citti, Donatella Peca, Stefania Petrini, Renato Cutrera, Paolo Biban, Cristina Haass, Renata Boldrini & Olivier Danhaive

To cite this article: Arianna Citti, Donatella Peca, Stefania Petrini, Renato Cutrera, Paolo Biban, Cristina Haass, Renata Boldrini & Olivier Danhaive (2013) Ultrastructural Characterization of Genetic Diffuse Lung Diseases in Infants and Children: A Cohort Study and Review, Ultrastructural Pathology, 37:5, 356-365, DOI: 10.3109/01913123.2013.811454

To link to this article: https://doi.org/10.3109/01913123.2013.811454

Ultrastructural Pathology, 2013; 37(5): 356–365

ISSN: 0191-3123 print / 1521-0758 online
DOI: 10.3109/01913123.2013.811454

informa
healthcare

ORIGINAL ARTICLE

Ultrastructural Characterization of Genetic Diffuse Lung Diseases in Infants and Children: A Cohort Study and Review*

Arianna Citti[1]*, Donatella Peca, PhD[2]*, Stefania Petrini, PhD[2], Renato Cutrera, MD[3], Paolo Biban, MD[4], Cristina Haass, MD[5], Renata Boldrini, MD[1], and Olivier Danhaive, MD[6,7]

[1]Division of Medical Pathology, [2]Research Core Laboratory, [3]Division of Pulmonology, Bambino Gesù Children's Hospital, Rome, Italy, [4]Neonatal and Pediatric Intensive Care Unit, Verona University Hospital, Verona, Italy [5]S. Pietro Fatebenefratelli Hospital, Rome, Italy, [6]Division of Neonatology, Bambino Gesù Children's Hospital, Rome, Italy, and [7]Division of Neonatology, University of California San Francisco, San Francisco, California, USA

ABSTRACT

Pediatric diffuse lung diseases are rare disorders with an onset in the neonatal period or in infancy, characterized by chronic respiratory symptoms and diffuse interstitial changes on imaging studies. Genetic disorders of surfactant homeostasis represent the main etiology. Surfactant protein B and ABCA3 deficiencies typically cause neonatal respiratory failure, which is often lethal within a few weeks or months. Although heterozygous ABCA3 mutation carriers are mostly asymptomatic, there is growing evidence that monoallelic mutations may affect surfactant homeostasis. Surfactant protein C mutations are dominant or sporadic disorders leading to a broad spectrum of manifestations from neonatal respiratory distress syndrome to adult pulmonary fibrosis. The authors performed pathology and ultrastructural studies in 12 infants who underwent clinical lung biopsy. One carried a heterozygous SP-B mutation, 3 carried SP-C mutations, and 7 carried ABCA3 mutations (5 biallelic and 2 monoallelic). Optical microscopy made it possible to distinguish between surfactant-related disorders and other forms. One of the ABCA3 monoallelic carriers had morphological features of alveolar capillary dysplasia, a genetic disorder of lung alveolar, and vascular development. One patient showed no surfactant-related anomalies but had pulmonary interstitial glycogenosis, a developmental disorder of unknown origin. Electron microscopy revealed specific lamellar bodies anomalies in all SP-B, SP-C, and ABCA3 deficiency cases. In addition, the authors showed that heterozygous ABCA3 mutation carriers have an intermediate ultrastructural phenotype between homozygous carriers and normal subjects. Lung biopsy is an essential diagnostic procedure in unexplained diffuse lung disorders, and electron microscopy should be performed systematically, since it may reveal specific alterations in genetic disorders of surfactant homeostasis.

Keywords: ABCA3, alveolar capillary dysplasia, pediatric diffuse lung disease, SP-B, SP-C, surfactant

Pediatric diffuse lung diseases (pDLD) are a heterogeneous group of rare disorders characterized by impaired gas exchange, diffuse infiltrates on imaging, and an onset in infancy [1]. Genetic disorders of surfactant synthesis and homeostasis represent an important subset of these diseases, and are caused by mutations in the genes encoding surfactant protein B (SP-B), surfactant protein C (SP-C), ATP-binding cassette transporter A3 (ABCA3), thyroid transcription factor 1 (TTF-1), and others. SP-B and SP-C are two hydrophobic proteins associated with surfactant phospholipids and play a critical role in surfactant tension active properties and homeostasis. Indeed, mutations in these two genes are associated with pDLD, while the other surfactant protein genes (SP-A and SP-D), encoding for collectin-like molecules, have

Received 15 April 2013; Revised 27 May 2013; Accepted 29 May 2013; Published online 17 September 2013

*Arianna Citti and Donatella Peca contributed equally to this work and share first authorship.

Correspondence: Dr Olivier Danhaive, UCSF San Francisco General Hospital, 1001 Potrero Avenue, mailstop 6E, San Francisco, CA 94110, USA. E-mail: danhaiveo@peds.ucsf.edu

not been clearly associated with pDLD so far. SP-B deficiency is caused by biallelic mutations with autosomal recessive transmission, and is associated with lethal respiratory distress syndrome (RDS) in term neonates [2]. SP-C mutations are typically monoallelic, 50% sporadic and 50% transmitted in autosomal dominant mode, are associated with a broad spectrum of clinical manifestations [3], including neonatal RDS, interstitial lung disease (ILD) in infants and children, familial pulmonary fibrosis in adults, recurrent infections, and bronchiectasis [4], and are also found in asymptomatic relatives of carriers, indicating a variable penetrance likely influenced by genetic and environmental factors. ABCA3 is a lipid transporter associated with lamellar bodies and critical for surfactant synthesis. Complete ABCA3 deficiency caused by biallelic homozygous or double heterozygous mutations typically leads to early-onset RDS similar to SP-B deficiency [5], but has also been associated with ILD in older children and adults, similar to SP-C mutations [6,7]. Although heterozygous carriers of ABCA3 mutations are considered as asymptomatic, single ABCA3 mutations have been described as disease modifiers, either isolated [8] or in compound heterozygosity with mutations in other surfactant genes [9]. TTF-1 is a nuclear factor that plays an essential role both in early lung embryogenesis and in lung epithelium maturation and surfactant synthesis, but also in thyroid and brain development and function. TTF-1 is a critical regulator of the expression of several other surfactant-related genes, including SP-B, SP-C, and ABCA3 [10]. Mutations or deletions causing haploinsufficiency of NKX2.1, the gene that encodes TTF-1, lead to variable combinations of respiratory failure, hypothyroidism and brain-related symptoms, such as choreoathetosis and hypopituitarism. Lung symptoms vary from early-onset lethal RDS to recurrent respiratory failure and ILD in older children and adults [11,12].

Another category of pDLDs of presumed genetic origin is developmental lung disorders, including alveolar capillary dysplasia with misalignment of pulmonary veins (ACD), acinar dysplasia, and congenital alveolar dysplasia, a group of rare diseases of alveolar and pulmonary vasculature development manifesting as persistent pulmonary hypertension and impaired gas exchange in full-term neonates [13]. ACD is caused in 40% of cases by monoallelic mutations and deletions of the FOXF1 gene and its regulatory region [14].

Neuroendocrine cell hyperplasia of infancy (NEHI) and pulmonary interstitial glycogenosis (PIG) represent other forms of pDLD in which a genetic origin is suspected but not identified. PIG manifests as acute progressive respiratory failure in newborn and infants, but had a more favorable prognosis with respect to other diffuse interstitial lung disease, and is amenable to steroid therapy [15,16]. NEHI is characterized by severe respiratory failure in newborn and infants not correlated with significant histological changes and usually reversible spontaneously [17].

Whereas optical histology provide limited insights in the precise etiologic diagnosis of genetic surfactant deficiencies, showing in most cases a nonspecific patterns of desquamative interstitial pneumonia and/or alveolar proteinosis, electron microscopy, even if an often limited resource, represents the gold standard instrument to identify such disorders, allowing researchers to orient molecular and genetic studies toward specific diagnoses and to differentiate them from alternative causes of pDLD [18]. The object of this article is to review the morphological and ultrastructural features of pDLD as observed in 12 infants and children with pDLD referred for diagnosis to the Bambino Gesù Children Hospital, IRCCS, Rome, Italy, a tertiary children's hospital, who underwent surgical lung biopsies and extensive molecular genetic characterization.

PATIENTS AND METHODS

Patients

We screened a cohort of 88 patients recruited from 2007 to 2012 with pDLD. The infants' ages ranged from birth to 18 years, with a prevalence of neonates. The inclusion criteria consisted of respiratory symptoms (abnormal auscultation, hypoxemia, cough, increased work of breathing) and diffuse lung disease on chest radiogram; children with an identified etiology (bronchopulmonary dysplasia of prematurity, lung hypoplasia, cystic fibrosis, lung bacterial, viral and fungal infections, ciliary dyskinesia, airway malformations, chronic aspiration, and structural heart defect) were excluded. Eligible patients underwent genetic testing and, with parental consent, surgical lung biopsy. Blood samples for genetic analysis were collected from the index patients and each direct family member; lung biopsies or autopsy specimens were obtained after informed parental consent. Lung tissue samples from peripheral areas of congenital cystic adenomatoid malformations (CCAM) patients were used as normal control.

DNA Sequence Analysis

Screening for sequence variations in the SP-B, SP-C, ABCA3, and TTF-1 encoding genes was performed by direct sequencing of PCR-amplified products from genomic DNA obtained from whole blood using the QIAamp DNA blood minikit (Qiagen, Australia), following the manufacturer's instructions. Polymerase chain reaction (PCR) amplifications were performed on genomic DNA under standard

conditions in a PTC 200 Peltier thermal cycler (MJ Research, Watertown, MA, USA). Oligonucleotides (purchased from Sigma) were derived from published sequences [5]. The amplified fragments were purified and directly sequenced on both strands using the CEQ DTCS Quick Start Kit (Beckman Coulter). Sequencing primers were the same as the ones used in amplification reactions. Sequencing products were analyzed on a CEQ200XL sequencer (Beckman Coulter). Parental DNA was sequenced when samples were available, and nonsynonymous mutations were analyzed in at least 50 healthy subjects (100 chromosomes).

Microscopical Studies

For optical microscopy, 5-μm lung tissue sections from formalin-fixed, paraffin-embedded samples obtained by open chest wedge biopsy and/or autopsy were stained with hematoxylin–eosin, periodic acid–Schiff (PAS), and Weigert-Van Gieson staining for standard histopathology. Ultrastructural studies were performed using open chest lung biopsy fragments. Samples were fixed in Karnowsky's fixative, postfixed in osmium tetroxide (OsO_4), and dehydrated up to absolute ethanol and embedded in EMbed-812. Ultrathin sections were stained with lead citrate and uranyl acetate and observed with a Zeiss EM CENTRA 100 transmission electron microscope (Carl Zeiss, Oberkochen, Germany) operated at 60 kV. Control lung tissue was obtained from a term newborn who underwent pulmonary lobectomy for congenital cystic adenoid malformation. In the subset of patients with ABCA3 mutations (patients 5–11), in order to obtain a semi-quantitative analysis of the respective ultrastructural phenotype of biallelic and monoallelic ABCA3 mutants, we determined the average number per section and diameter of lamellar bodies (LB) in 10 randomly selected sagittal sections of alveolar epithelial type II cells (AEC2) for each case and controls.

RESULTS

In 12 of the eligible patients, surgical lung biopsies were performed and analyzed by optical (OM) and electronic (EM) microscopy. Seven were males and 5 were females, with an age of 1–25 months. Patient 1 had respiratory failure at 1 month of age requiring surfactant administration, and was discharged home at 6 months on oxygen, steroids, and bronchodilators. Patient 2 declared with hypoxemia at 1 month, required mechanical ventilation from 3 months, and died at 6 months; patients 3 and 4 became symptomatic at 6 months with persistent hypoxemia following a bronchiolitis episode; patient 3 died at 19 months; and patient 4 went home on oxygen and steroids at 13 months. Patients 5–9 were all term newborns presenting with unexplained respiratory distress syndrome within the first week of life, requiring mechanical ventilation and multiple therapeutic surfactant administration, and died between 3 and 9 months of age. Patient 10 presented with severe RDS and persistent pulmonary hypertension at birth but could be discharged home on room air at 3 months, then developed hypothyroidism and had recurrent respiratory failure episodes. Patient 11 had persistent hypoxemia since the first week of like, did not require mechanical ventilation, but developed severe pulmonary hypertension and died at 8 months. Patient 12 declared with hypoxemia and interstitial lung disease at 3 months, and went home at 6 months on room air after steroid treatment.

Genetic Findings

One patient (patient 1) carried a heterozygote mutation (121ins2) of the *SP-B* gene. Three patients (2–4) were heterozygous carriers of a *SP-C* mutation (E66K, I73T, and V102M, respectively), Seven patients were *ABCA3* mutation carriers: 5 patients (5–9) carried biallelic mutations (c3997delA in homozygosis and the double heterozygous compounds R208W/T1423I, R43L/R1482W, P147L/R155Q, and P248L/L941P, respectively); 2 patients (10, 11) carried only a single mutation (L941P and A501E). In the last patient (12) no mutations were found.

Morphological Aspects

In patient 1 (monoallelic SP-B mutant), OM analysis revealed abnormal accumulation of eosinophilic granular material in the alveolar lumen positive to periodic acid–Schiff staining, AEC2 hyperplasia, and interalveolar septum thickening with fibroblast proliferation (Figure 2A), a pattern initially described as pulmonary alveolar proteinosis (PAP) in the literature, although significantly different from the classic, autoimmune PAP found in adults or the congenital form caused by CSF2RA/B deficiency [19]. EM analysis showed, both in the AEC2 cytoplasm and in the proteinaceous exudate in alveolar lumen, clusters of multivesicular bodies and/or composite bodies (Figure 2B, C), in absence of the well-organized concentric rings of phospholipid membrane normally present in lamellar bodies (Figure 1B, C).

In patients 2–4 (monoallelic SP-C mutants), OM features were characterized by scattered areas of interalveolar septum thickening with inflammatory infiltrates, fibroblast proliferation, and collagen deposition, plus mixed amorphous and cellular content in alveolar spaces with some degree of AEC2 hyperplasia (Figure 3A), a pattern corresponding to

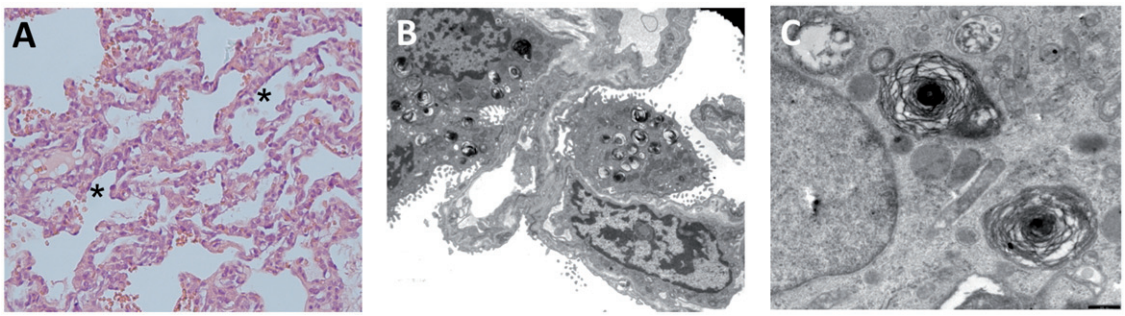

FIGURE 1. Normal lung tissue from a 4-week-old infant with lung congenital cystic adenomatoid malformation. (A) Low-power optical microscopy (OM) showing clear alveolar spaces lined with type I and type II epithelial cells, thin interalveolar septi. Hematoxylin–eosin (HE), 20×). (B) Low-magnification electron microscopy (EM) showing two type II alveolar cells facing contiguous alveoli, with abundant lamellar bodies and pseudomyelin appearance of surfactant content (2000×). (C) High magnification of normal lamellar bodies, showing concentric phospholipid membranes (pseudomyelin) (10,000×).

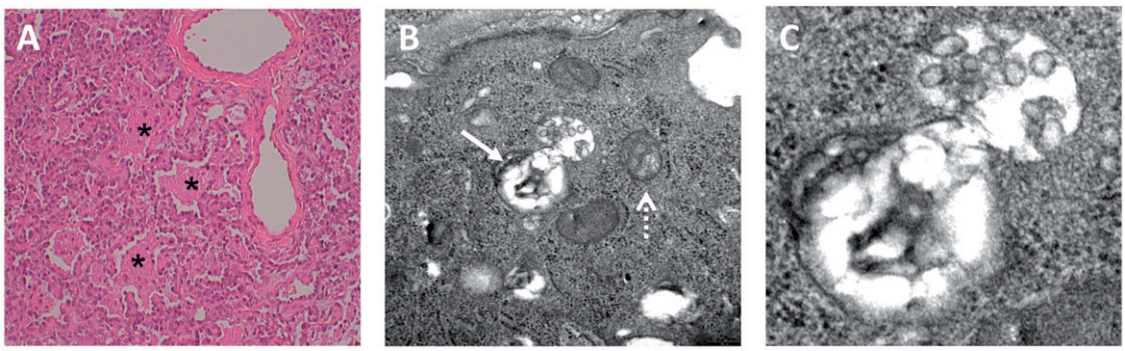

FIGURE 2. Lung tissue from heterozygous SP-B mutation carrier (patient 1). (A) Low-magnification OM showing alveolar spaces (*) lined almost exclusively with type 2 epithelial cells (cuboid metaplasia) and filled with amorphous fluid and few cellular elements, corresponding to a mixed picture of desquamative interstitial pneumonia and pulmonary alveolar proteinosis (HE, 20×). (B) Medium-magnifcation EM showing one type II epithelial cell with enlarged lamellar bodies containing destructured surfactant membranes and no visible pseudomyelin (arrow), plus abundant multivesicular bodies (dashed arrow) and hypertrophic endoplasmic reticulum. (C) High magnification of a lamellar body fusing with a multivesicular body.

nonspecific interstitial pneumonia (NSIP) and diffuse interstitial pneumonia (DIP), found in different forms of ILD in infants and children, and more age- than disease-specific. Electron microscopy revealed mixed appearance of LB, ranging from normal to enlarged with no identifiable pseudomyelin layers and containing electron-dense vesicles and disorganized membranous aggregates (Figure 3B, C); in addition, our patients showed large cytoplasmic vacuoles corresponding to early endosomes, and vesicular organelles containing electron-dense material likely corresponding to aggresomes (Figure 3D).

In patients 5–9 (biallelic ABCA3 mutants), OM revealed diffuse AEC2 hyperplasia (Figure 4B), diffuse cell and amorphous material accumulation in the alveolar lumen, and interalveolar septum fibroblast proliferation and fibrosis (Figure 4A), reported as DIP or, improperly, PAP in the literature. One patient (7) was characterized predominantly by alveolar, PAS-positive lipoproteinaceous material accumulation plus macrophages and desquamated epithelial cells (data not shown), a pattern more similar to PAP. Patients 10 and 11 (monoallelic ABCA3 mutants) (Figure 4C) were not significantly distinct from those patients with biallelic mutants (Figure 4D, E). EM examination showed the presence of small, markedly abnormal lamellar bodies with densely packed phospholipid membranes or cristalline structures and one or two electron-dense inclusions, designated ''fried egg.'' The number of these fried egg LB varied according to the type of molecular defect, from absent/rare in biallelic frameshift mutation to numerous in certain biallelic missense mutations, whereas in subjects with monoallelic mutations a mix of fried egg and normal LB was observed. Biallelic mutants ($n = 5$) have a smaller average LB number ($p < 0.01$) with a smaller average diameter ($p < 0.01$) than controls ($n = 3$); monoallelic mutants ($n = 2$) showed an average LB number greater than biallelic carriers ($p < 0.05$) similar to controls, but a smaller average diameter than controls ($p < 0.05$), similar to biallelic carriers (Figure 5).

In addition to her monoallelic ABCA3 mutation, patient 11's OM analysis revealed a marked reduction in pulmonary capillary density in the alveolar septa failing to make contact with the alveolar basal

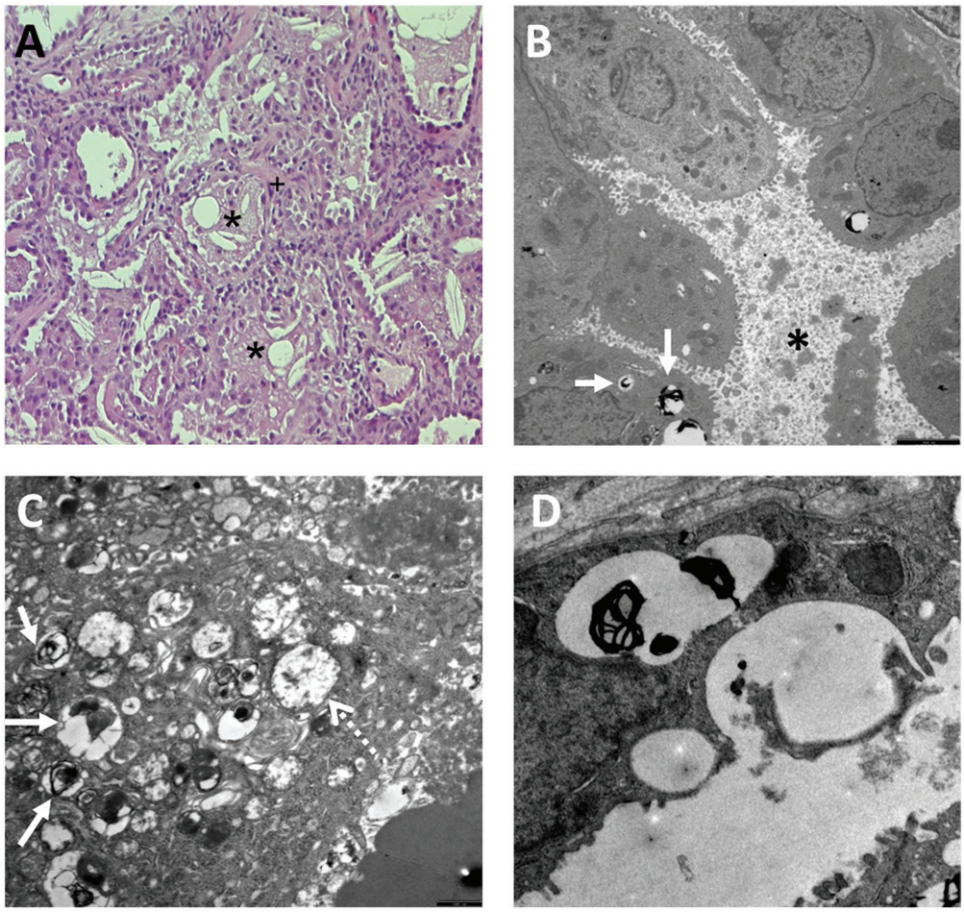

FIGURE 3. Lung tissue from SP-C heterozygous carrier (patient 2). (A) Low-magnification OM showing alveolar spaces (*) with some degree of cuboid metaplasia, to a lesser extent than in SP-B deficiency, mostly filled with amorphous fluid and abundant cellular elements, and interstitial fibroblast proliferation and collagen deposition (+), corresponding to desquamative interstitial pneumonia (HE, 20×). (B) Low-magnification EM showing an alveolar space (*) filled with heterogeneous material and a macrophage, and lined predominantly with alveolar type II cells containing few abnormal lamellar bodies (arrows). (C) Medium-magnification EM of a type II epithelial cell showing enlarged lamellar bodies containing disorganized lamellar structures (arrows) plus large endosomes (dashed arrow) (6000×). (D) High-power EM showing enlarged lamellar bodies with abnormal phospholipid content secreted in the alveolar lumen (9000×).

membrane, plus increased muscularization of the small arterioles and pulmonary veins adjacent to the pulmonary arteries in the same adventitial sheath (Figure 6A) and intraalveolar septi with internalized capillary vessels (Figure 6B), a set of features consistent with the diagnosis of ACD. We retrospectively screened for FOXF1 point mutations and microdeletions but did not find any variations. A mixed ultrastructural phenotype could be observed in this patient, including fried egg inclusions in AEC2 typical of ABCA3 deficiency (Figure 6C).

In patient 12, in whom no surfactant-related genetic defect could be identified, OM analysis showed enlarged interalveolar septa with PAS-positive (Figure 7A) and diastase-sensitive material (not shown) within the cytoplasm of mesenchymal cells, indicating the presence of glycogen. At the ultrastructural level, these interstitial cells had features of primitive mesenchymal cells with vacuolized cytoplasm (Figure 7B, C). Overall, these features are typical of pulmonary interstitial glycogenosis (PIG).

DISCUSSION

Ultrastructural Aspects of the Normal Lung

Pulmonary surfactant is synthesized exclusively by AEC2, which represent about 60% of alveolar epithelial cells but appeared scattered and protruding among flat type I cells, given their cuboid shape with a much smaller basal surface. Mature AEC2 are characterized by apical microvilli and LB, cell-specific organelles clustered at the apical portion of the cytoplasm and containing the intra-cellular surfactant pool appearing as onion skin-like regular concentric lamellae, with a pattern often designated pseudomyelin [20]. Around birth, AEC2 are characterized by a higher LB and mitochondrial number than in mature subjects,

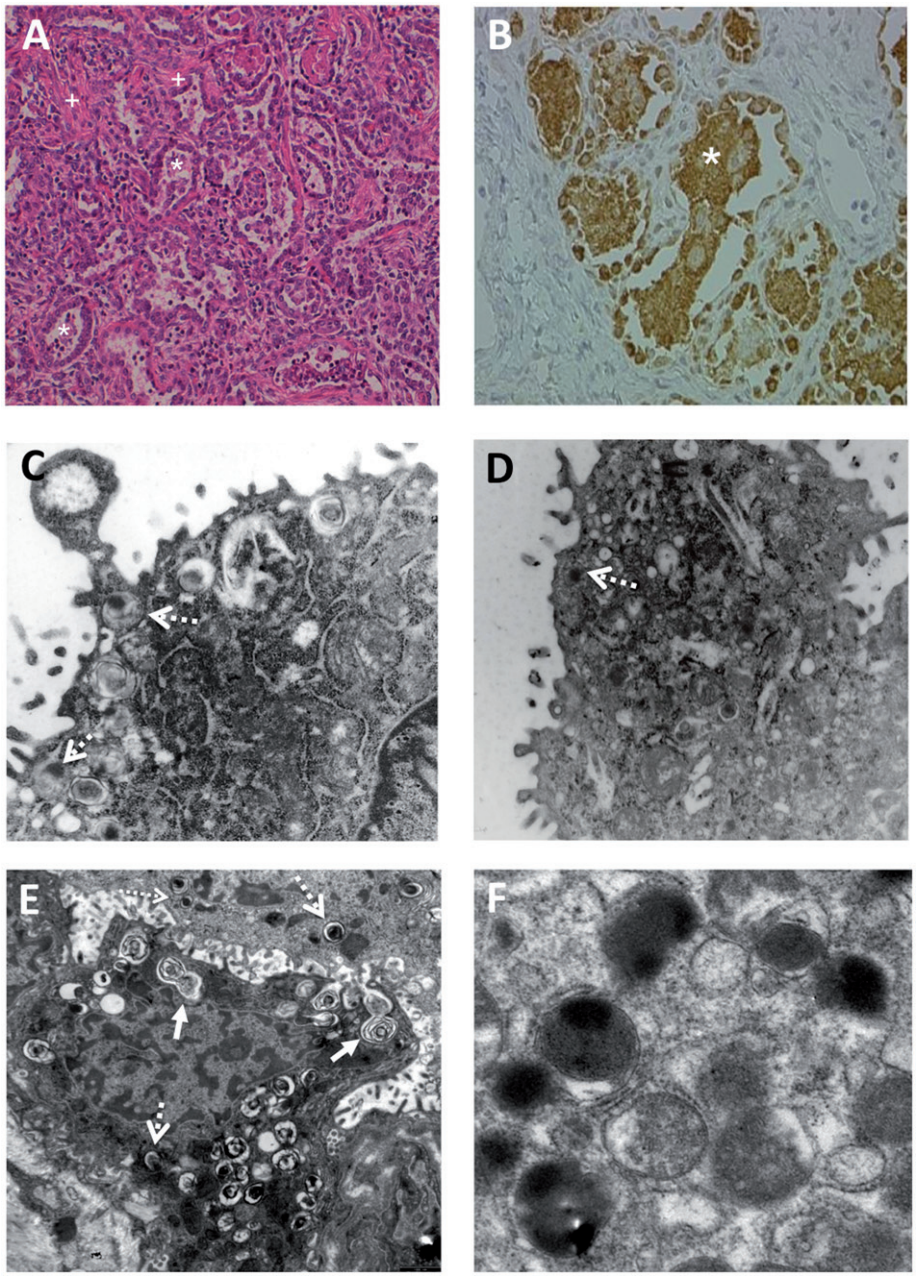

FIGURE 4. Lung tissue from ABCA3 mutation carriers. (A) Low-magnification OM of a homozygous carrier (patient 5) showing alveolar spaces (*) with near-total cuboid metaplasia, filled with amorphous fluid and abundant cellular elements, plus interstitial fibroblast proliferation and collagen deposition (+), corresponding to desquamative interstitial pneumonia (HE, 20×). (B) Immunohistochemistry staining with an anti-SP-B antibody, showing alveoli lined exclusively with type II cells and intraalveolar surfactant protein accumulation and macrophages (IHC, 40×). (C) High-magnification EM of a homozygous carrier (patient 5) showing rarefied, small lamellar bodies (dashed arrows) with no visible pseudomyelin (9000×). (D) High-magnification EM of a biallelic double heterozygous carrier (#6) showing similar rarefied, small lamellar bodies (dashed arrows) with no visible pseudomyelin (9000×). (E) Low-magnification EM of a monoallelic, heterozygous carrier (patient 10) showing a mix of normal-appearing lamellar bodies (arrows) and small amorphous lamellar bodies (dashed arrow) in a neighboring cell. (F) High-power EM of a cluster of lamellar bodies in a homozygous carrier (patient 5) with densely packed membranes and denser cores, designated ''fried eggs''.

whereas immature AEC2 show abundant cytoplasmic glycogen pools and less numerous LB [21].

SP-B Deficiency

SP-B deficiency is an extremely rare autosomal recessive disorder, with an estimated prevalence $<1/10^6$ live births, usually lethal in the first weeks of life, whereas heterozygous carriers are asymptomatic. In optical microscopy SP-B deficiency is characterized by widened interstitium with fibroblast proliferation, arrested acinar development with reduced alveolar number, cuboid metaplasia of the alveolar epithelium, and alveolar lumen filled with eosinophilic

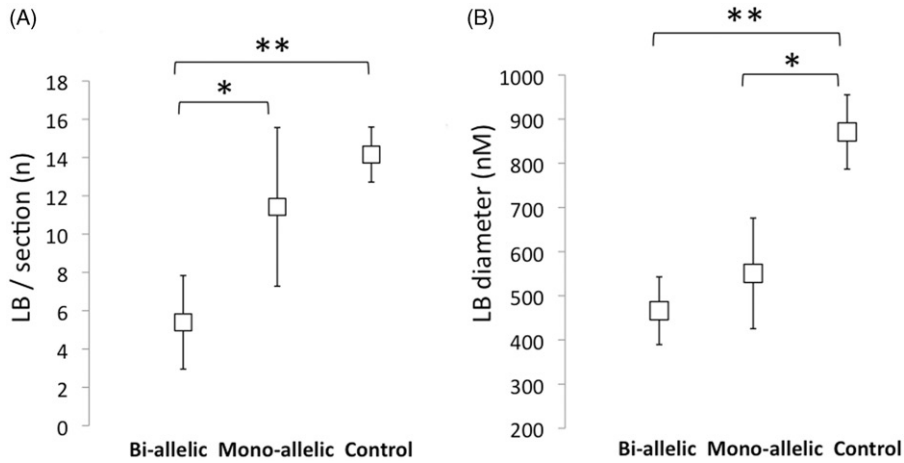

FIGURE 5. Comparision of lamellar body density and size in biallelic and monoallelic ABCA3 mutation carriers. (A) Average lamellar body number per cell saggital section (10 sections/case) in biallelic carriers ($n = 5$), monoallelic carriers ($n = 2$), and controls ($n = 3$). *$p < 0.05$; **$p < 0.01$. (B) Average lamellar body diameter (nm) in biallelic carriers ($n = 5 \times 10$ sections), monoallelic carriers ($n = 2$), and controls ($n = 3$). *$p < 0.05$; **$p < 0.01$.

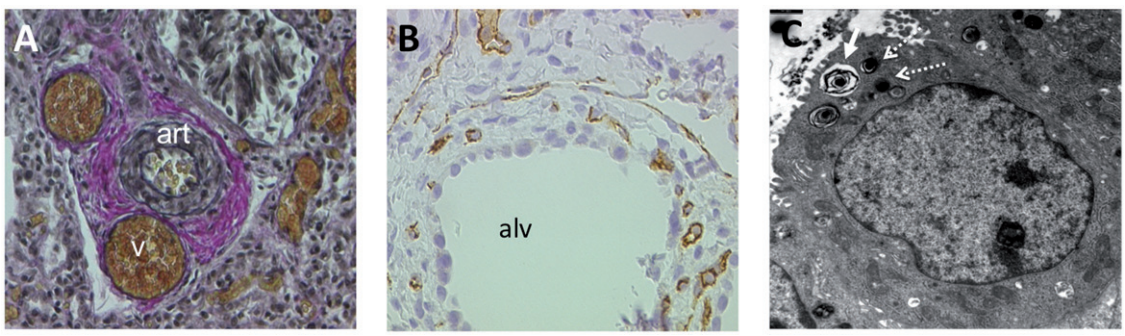

FIGURE 6. Lung tissue from patient with alveolar capillary dysplasia and heterozygous ABCA3 mutation carrier (patient 11). (A) High-magnification OM showing a pulmonary arteriole (art) with thickened media, with two pulmonary venules (v) running parallel to the artery in the same adventitial sheath. Weigert-Van Gieson staining, 40×. (B) Immunohistochemistry staining with anti-CD31 antibody, showing decreased density of pulmonary capillaries that fail to make contact with the alveolar basal membrane (40×). (C) Medium-power EM showing a mix of normal (arrow) and fried egg lamellar bodies (dashed arrow).

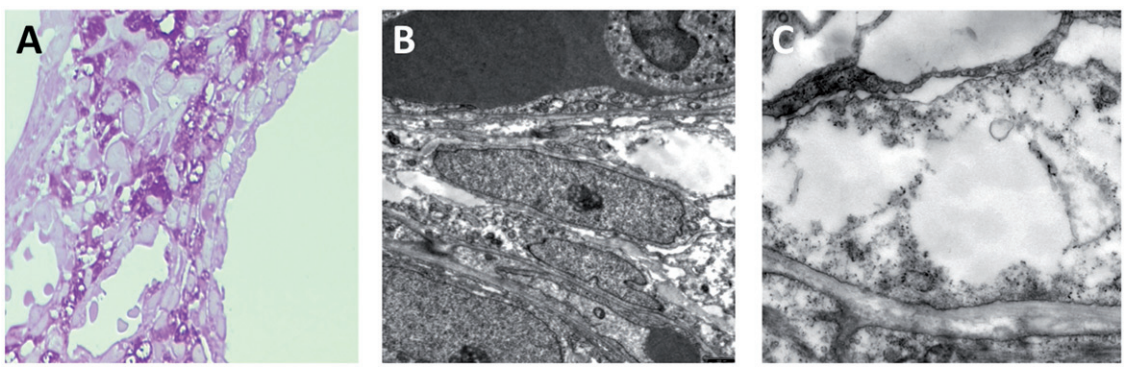

FIGURE 7. Pulmonary interstitial glycogenosis (patient 12). (A) OM showing enlarged interalveolar septa with PAS-positive material within the cytoplasm of mesenchymal cells, corresponding to glycogen. (B) Medium-power EM showing intracellular glycogen deposits (6000×). (C) Monoparticulate glycogen deposits (12,000×).

proteinaceous material containing macrophages and desquamated clusters of epithelial cells, a pattern described as DIP, although it was often reported as PAP in the former literature [22]. LB morphology and the ultrastructural features of intracellular surfactant are very distinctive: normal, mature LB with well-organized pseudomyelin structures are not present, and are replaced by larger cytoplasmic inclusion with irregularly disposed lamellae and multiple associated membranous and vesicular structures [23].

These findings are compatible with animal studies, where SP-B-deficient mice are characterized by high neonatal mortality, a complete absence of LB, and the presence of inclusions containing numerous small vesicles and electron-dense masses in AEC2 [24]. Although our case is a heterozygote carrier of the 121ins2 mutation and the clinical phenotype was milder than that typically reported for homozygous carriers, ultrastructural features were typical of SP-B deficiency and suggest the presence of an unidentified mutation in the second allele [25].

SP-C Deficiency

SP-C deficiency is clinically the most heterogeneous defect of surfactant homeostasis. Mutations in SP-C range from fatal pulmonary surfactant deficiency to pediatric interstial lung disease and to adult familial/idiopathic pulmonary fibrosis, with asymptomatic carriers being described in affected families. Most SP-C mutations cluster in the noncoding C-terminal part of the proSP-C apoprotein and lead to misfolding protein cell response, amyloid formation, and epithelial cell apoptosis (BRICHOS mutations) or to mistrafficking to the endosomal compartment and intraalveolar abnormal apoprotein products accumulation (non-BRICHOS mutations) [26]. Lung morphology in SP-C deficiency is characterized by diffuse alveolar damage, interstitial thickening with fibroblast proliferation and collagen deposition, abundant foamy alveolar macrophages and granular lipoproteic material in the alveolar lumen, and AEC2 hyperplasia, corresponding to DIP, albeit with a more scattered, multifocal pattern, multiple fibrosis foci and an overall broader variability between subjects that in SP-B deficiency [27]. Surprisingly, in the complete SP-C deficiency mouse model, the number of AEC2 was similar compared to wild type and well-organized lamellar bodies were detected. However, lung mechanics studies showed a lower lung compliance at the end-expiratory pressure and increased sensitivity to lung injury, suggesting that SP-C stabilizes the phospholipid film at reduced lung volumes [28].

ABCA3 Deficiency

In our cohort, as in several other published series [5,29,30], ABCA3 deficiency was the most common defect. Infants with ABCA3 mutations have a spectrum of clinical presentation and lung morphology alterations similar to those with either SP-B or SP-C mutations, but ultrastructural examination of AEC2 demonstrates distinctive features, consisting of abnormal LB with tightly packed concentric membranes and an aggregate of electron-dense material (fried egg appearance) [23]. ABCA3-deleted mice have a similar phenotype to humans, with fried egg and low number LB [31], and resulted in respiratory failure after birth. ABCA3 is located in LB membranes and involved in intracellular lipid transport and intracellular surfactant packaging. Although ABCA3 deficiency is typically described as an autosomal recessive disorder with healthy heterozygous carriers, some recent data suggest that monoallelic mutations affect surfactant homeostasis and may cause or alter the course of lung disease in infants [7]. The mixed ultrastructural phenotype we observed in two single mutation carriers, consisting of LB numbers similar to controls but diameters similar to biallelic (homozygous or double heterozygous) mutants, suggests that partial ABCA3 deficiency affects surfactant homeostasis and therefore can be at least partially responsible for the clinical phenotype.

Alveolar Capillary Dysplasia (ACD)

ACD is a rare disorder of early lung development of unknown pathogenesis, leading to defective angiogenesis and alveolar development, the molecular mechanisms of which are still largely unknown. Genetically, ACD is a heterogeneous disease, since FOXF1 variants could not be demonstrated in more than half the published cases. Histologically, it is characterized by a scattered pattern of interalveolar septal thickening, decreased terminal bronchial ramification and alveolar number, increased muscularization in small pulmonary arteries, misalignment of pulmonary veins along small pulmonary arteries, and decreased capillary number failing to make an appropriate contact with the alveolar basal membrane, leading to pulmonary hypertension and impaired gas exchange [32]. In more than 50% cases ACD is associated with malformations in other organs involving the gastrointestinal, cardiovascular, and genitourinary systems, suggesting a more pervasive embryonic process [33]. ACD is best diagnosed by optical microscopy, showing the specific morphological features described above; reduced capillary density can be further evidenced by immunohistochemestry techniques using endothelial marker antibodies, such as CD31 or VFGE. EM can be used to demonstrate capillary internalization, but is also important for differential diagnosis, showing the integrity of the surfactant system or, as in our case, the presence of an associated surfactant gene defect [34].

Pulmonary Interstitial Glycogenosis (PIG)

PIG is an extremely rare and possibly underrecognized disease of unknown etiology, which causes respiratory failure in newborns and can be associated

with congenital heart disease and persistent pulmonary hypertension. Although its histological hallmark consists of thickened interstitium with immature interstitial cells containing intracytoplasmic glycogen, PIG is not linked to deficiency of enzymes related to glycogen metabolism, but is believed to correspond to a maturation deficiency of the interstitial fibroblasts. Ultrastructural studies show primitive intestitial cells with few organelles and abundant monoparticulate glycogen, whereas no abnormal glycogen accumulation can be seen in AEC2. PIG has been shown to respond clinically to corticosteroid therapy, suggesting that this defect can be reversed by inducing and accelerating interstitial cell maturation [35]. No genetic etiology has been identified so far. Some authors consider PIG to be a disorder of alveolar growth, since it can also be observed as a focal lesion adjacent to masses or cystic lesions, or in exacerbation phases of chronic lung disease of prematurity [36].

CONCLUSION

The clinical and anatomopathological overlap of congenital diffuse lung disorders makes ultrastructural examination essential for establishing the diagnosis of surfactant homeostasis disorder in patients with suggestive, unexplained phenotypes. Moreover, AEC2 ultrastructural analysis may allow identification of or suggest the genetic defect underlying the disease and permit faster and more specific molecular testing. Hence, surgical lung biopsy should be recommended in infants and children with unexplained pDLD, and should always include proper samples for ultrastructural analysis.

DECLARATION OF INTEREST

The authors report no conflicts of interest. The authors alone are responsible for the content and writing of the paper.

This publication was supported by an unrestricted grant by the Chiesi Foundation, Parma, Italy, and by an institutional grant from the Italian Ministry of Health.

REFERENCES

1. Deutsch GH, Young LR, Deterding RR, et al; Pathology Cooperative Group; Child Research Co-operative. Diffuse lung disease in young children: application of a novel classification scheme. *Am J Respir Crit Care Med* 2007;177: 1120–8.
2. Nogee LM, Garnier G, Dietz HC, et al. A mutation in the surfctant protein B gene rsponsible for fatal neonatl respiratory disease in multiple kindreds. *J Clin Invest* 1994;93: 1860–3.
3. Guillot L, Epaud R, Thouvenin G, et al. New surfactant protein C mutations associated with diffuse lung disease. *J Med Genet* 2009;46: 490–4.
4. Salerno T, Peca D, Rossi FP, et al. Bronchiectasis and severe respiratory insufficiency associated with a new surfactant protein C mutation. *Acta Paediatr* 2013;102: e1–2.
5. Shulenin S, Nogee LM, Annilo T, et al. ABCA3 gene mutations in newborns with fatal surfactant deficiency. *N Engl J Med* 2004;350: 1296–303.
6. Bullard JE, Wert SE, Whitsett JA, et al. ABCA3 mutations associated with pediatric interstitial lung disease. *Am J Respir Crit Care Med* 2005;172: 1026–31.
7. Young LR, Nogee LM, Barnett B, et al. Usual interstitial pneumonia in an adolescent with ABCA3 mutations. *Chest* 2008;134: 192–5.
8. Wambach JA, Wegner DJ, Depass K, et al. Single ABCA3 mutations increase risk for neonatal respiratory distress syndrome. *Pediatrics* 2012;130: e1575–82.
9. Bullard JE, Nogee LM. Heterozygosity for ABCA3 mutations modifies the severity of lung disease associated with a surfactant protein C gene (SFTPC) mutation. *Pediatr Res* 2007;62: 176–9.
10. Besnard V, Xu Y, Whitsett JA. Sterol response element binding protein and thyroid transcription factor-1 (Nkx2.1) regulate Abca3 gene expression. *Am J Physiol Lung Cell Mol Physiol* 2007;293: L1395–405.
11. Hamvas A, Deterding RR, Wert SE, et al. Heterogeneous pulmonary phenotypes associated with mutations in the thyroid transcription factor gene NKX2-1. *Chest* 2013; [epub ahead of print], doi: 10.1378/chest.12-2502.
12. Peca D, Petrini S, Tzialla C, et al. Altered surfactant homeostasis and recurrent respiratory failure secondary to TTF-1 nuclear targeting defect. *Respir Res* 2011;12: 115.
13. Bishop NB, Stankiewicz P, Steinhorn RH. Alveolar capillary dysplasia. *Am J Respir Crit Care Med* 2011;184: 172–9.
14. Sen P, Yang Y, Navarro C, et al. Novel FOXF1 mutations in sporadic and familial cases of alveolar capillary dysplasia with misaligned pulmonary veins imply a role for its DNA binding domain. *Hum Mutat* 2013;34: 801–11.
15. Canakis AM, Cutz E, Manson D, O'Brodovich H. Pulmonary interstitial glycogenosis: a new variant of neonatal interstitial lung disease. *Am J Respir Crit Care Med* 2002;165: 1557–65.
16. King BA, Boyd JT, Kingma PS. Pulmonary maturational arrest and death in a patient with pulmonary interstitial glycogenosis. *Pediatr Pulmonol* 2011;46: 1142–5.
17. Deterding RR, Pye C, Fan LL, Langston C. Persistent tachypnea of infancy is associated with neuroendocrine cell hyperplasia. *Pediatr Pulmonol* 2005;40: 157–65.
18. Wert SE, Whitsett JA, Nogee LM. Genetic disorders of surfactant dysfunction. *Pediatr Dev Pathol* 2009;12: 253–74.
19. Suzuki T, Sakagami T, Young LR, et al. Hereditary pulmonary alveolar proteinosis: pathogenesis, presentation, diagnosis, and therapy. *Am J Respir Crit Care Med* 2010;182: 1292–304.
20. Fehrenbach H. Alveolar epithelial type II cell: defender of the alveolus revisited. *Respir Res* 2001;2: 33–46.
21. Snyder JM, Magliato SA. An ultrastructural, morphometric analysis of rabbit fetal lung type II cell differentiation in vivo. *Anat Rec* 1991;229: 73–85.
22. Nogee LM, de Mello DE, Dehner LP, Colten HR. Brief report: deficiency of pulmonary surfactant protein B in congenital alveolar proteinosis. *N Engl J Med* 1993;328: 406–10.
23. Edwards V, Cutz E, Viero S, et al. Ultarstructure of lamellar bodies in congenital surfactant deficiency. *Ultrastruct Pathol* 2005;29: 503–9.

24. Stahlman MT, Gray MP, Falconieri MW, et al. Lamellar body formation in normal and surfactant protein B-deficient fetal mice. *Lab Invest* 2000;80: 395–403.
25. Rossi FP, Salerno T, Peca D, et al. Interstitial lung disease in a child heterozygous for the 1549C→GAA (121ins2) mutation of surfactant protein B. *Eur Respir J* 2011;38: 985–7.
26. Woischnik M, Sparr C, Kern S, et al. A non-BRICHOS surfactant protein c mutation disrupts epithelial cell function and intercellular signaling. *BMC Cell Biol* 2010; 11: 88.
27. Hartl D, Griese M. Interstitial lung disease in children—genetic background and associated phenotypes. *Respir Res* 2005;6: 32.
28. Glasser SW, Burhans MS, Korfhagen TR, et al. Altered stability of pulmonary surfactant in SP-C-deficient mice. *Proc Natl Acad Sci U S A* 2001;98: 6366–71.
29. Somaschini M, Nogee LM, Sassi I, et al. Unexplained respiratory distress due to congenital surfactant deficiency. *J Pediatr* 2007;150: 649–53.
30. Garmany TH, Wambach JA, Heins HB, et al. Population and disease-based prevalence of the common mutations associated with surfactant deficiency. *Pediatr Res* 2008;63: 645–9.
31. Cheong N, Zhang H, Madesh M, et al. ABCA3 is critical for lamellar body biogenesis in vivo. *J Biol Chem* 2007;282: 23811–17.
32. Tiozzo C, Carraro G, Al Alam D, et al. Mesodermal Pten inactivation leads to alveolar capillary dysplasia-like phenotype. *J Clin Invest* 2012;122: 3862–72.
33. Stankiewicz P, Sen P, Bhatt SS, et al. Genomic and genic deletions of the FOX gene cluster on 16q24.1 and inactivating mutations of FOXF1 cause alveolar capillary dysplasia and other malformations. *Am J Hum Genet* 2009; 84: 780–91.
34. Danhaive O, Peca D, Boldrini R. ABCA3 mutation and pulmonary hypertension: a link with alveolar capillary dysplasia? *J Pediatr* 2008;152: 891–2.
35. Das S, Langston C, Fan LL. Interstitial lung disease in children. *Curr Opin Pediatr* 2011;23: 325–31.
36. Dishop MK. Diagnostic pathology of diffuse lung disease in children. *Pediatr Allergy Immunol Pulmonol* 2010;23: 69–85.